European Radiology (2019) 29:1248–1257
https://doi.org/10.1007/s00330-018-5622-9

MUSCULOSKELETAL

The effect of tube voltage combination on image artefact and radiation dose in dual-source dual-energy CT: comparison between conventional 80/140 kV and 80/150 kV plus tin filter for gout protocol

Ji Young Jeon[1] · Sheen-Woo Lee[1] · Yu Mi Jeong[1] · Han Joo Baek[2]

Received: 9 May 2018 / Revised: 8 June 2018 / Accepted: 19 June 2018 / Published online: 9 July 2018

Abstract

Objectives In dual-source CT, dual-energy (DE) performance is affected by various X-ray tube voltage combinations with and without tin filter (Sn). The purpose of this study was to assess the utility of the 80/150 Sn kV voltage combination in terms of image artefact and radiation dose for DECT gout protocol, compared with the conventional 80/140 kV.

Methods Seventy-four patients with suspected gout who underwent dual-source DECT examinations scanned at 80/140 kV (n = 37) and at 80/150 Sn kV (n = 37) were included. Patients' age, sex, and serum uric acid levels were matched between the two groups. The types and incidence of image artefacts and radiation dose were evaluated.

Results The 80/150 Sn kV group had significantly fewer patients with artefacts, compared to the 80/140 kV group [11 (30 %) of 37 vs 35 (94.6 %) of 37, $p < 0.001$]. Except for the motion artefact, the rest of the artefacts—skin, nail bed, submillimetre, motion, vascular, beam-hardening, clumpy artefact along tendon—were significantly less observed in the 80/150 Sn kV acquisitions. The dose-length product (DLP) and effective dose were significantly lower for the 80/150 Sn kV acquisitions compared with the 8s0/140 kV scans (DLP: 104.46 ± 10.66 mGy·cm vs 344.70 ± 56.39 mGy·cm, $p < 0.001$; effective dose: 1.04 ± 0.11 mSv vs 3.45 ± 0.56 mSv, $p < 0.001$).

Conclusions The 80/150 Sn kV voltage combination in dual-source DECT system could be used as one of the artefact reduction methods while reducing radiation dose for gout protocol when compared to the conventional 80/140 kV.

Key Points

- *DECT has emerged as the leading modality for non-invasive diagnosis of gout.*
- *Various X-ray tube voltage combinations are now feasible in dual-source DECT.*
- *The 80/150 Sn kV acquisition could facilitate artefact reduction in gout protocol.*

Keywords Gout · Tomography, X-ray computed · Tin · Artefacts · Radiation dosage

Abbreviations

ACR/EULAR	American College of Rheumatology/ European League Against Rheumatism
CT	Computed tomography
CTDIvol	CT dose index
DE	Dual-energy
DLP	Dose-length-product
DSCT	Dual-source CT
MSU	Monosodium urate monohydrate

✉ Ji Young Jeon
mdjeonjy@gmail.com

[1] Department of Radiology, Gil Medical Center, Gachon University College of Medicine, 21 Namdong-daero, 774beon-gil, Namdong-gu, Incheon 21565, Republic of Korea

[2] Division of Rheumatology, Department of Internal Medicine, Gil Medical Center, Gachon University College of Medicine, 21 Namdong-daero, 774beon-gil, Namdong-gu, Incheon 21565, Republic of Korea

Introduction

Gout is a true crystal deposition arthropathy caused by deposition of monosodium urate monohydrate (MSU) into joints and periarticular soft tissues. Dual-energy (DE) computed tomography (CT) is a non-invasive method to confirm the presence of MSU crystal deposits which aids the diagnosis of gout [1–6]. Various DECT scanning techniques can be used for gout

imaging [4, 7–10]: dual source-dual detector (Somatom Definition Flash, Definition Force; Siemens Healthineers, Erlangen, Germany), single source-rapid kilovoltage switching (Gemstone Spectral Imaging; GE Healthcare, Chicago, IL, USA), single-source multi-layered detector (iQon Spectral CT; Philips Healthcare, Best, The Netherlands), single-source sequential gantry rotations at different kilovoltage peaks (Aquilion ONE ViSION; Toshiba, Tokyo, Japan), single-source split-beam filter at target with a single detector ("TwinBeam") (Somatom Definition Edge; Siemens Healthineers) and single-source two successive spiral scans at different kilovoltage peaks (Somatom Definition AS, Definition Perspective; Siemens Healthineers). The overall sensitivity and specificity of DECT for gout have been reported to be greater than 0.8 in both the active gout and long-standing tophaceous gout [11–13]. On the basis of reliable published data and diagnostic accuracy, DECT has been included in the 2015 American College of Rheumatology/European League Against Rheumatism (ACR/EULAR) Collaborative Initiative Classification Criteria for Gout [14]. According to the 2015 ACR/EULAR classification criteria, for DECT, urate deposition is defined as the presence of color-coded urate at articular or periarticular sites. Images should be acquired using a DECT scanner, with data acquired at 80 kV and 140 kV and analysed using a two-material decomposition algorithm designed for gout that colour-codes urate [14]. However, not all material colour coded as urate on DECT images corresponds to actual urate deposition. Various types of DECT artefacts which have the potential to lead to a false-positive result on gout protocol have been reported [5, 15–19]. Recently, in dual-source CT (DSCT) system with two separate X-ray sources, it has been shown that DE acquisition with 80 kV and 150 kV plus tin filtration (80/150 Sn kV) has a better DE spectral separation than that with 80 kV and 140 kV (80/140 kV) [20]. Therefore, we hypothesised that the 80/150 Sn kV tube voltage combination in DSCT would be beneficial for improving artefacts in the clinical field if applied to DECT gout applications. Thus, the purpose of this study was to assess the utility of the 80/150 Sn kV voltage combination in terms of image artefact for DECT gout protocol compared with the conventional 80/140 kV. In addition, radiation dose between the two groups was also compared to evaluate patient's radiation exposure.

Materials and methods

Patients

This retrospective study was approved by our institutional review board and the requirement for informed consent was waived. In our institution, upper or lower extremity DECT depending on the symptomatic location has been performed of patients with suspected gout.

We electronically searched the patients who performed imaging with DECT gout protocol obtained at 80/150 Sn kV from January 2017 (introduction of 80/150 Sn kV combination) to December 2017. This initial search found out 46 DECT images. Among them, nine patients scanned the area of hand/wrist, knee or elbow were excluded. Thus, 37 patients who had undergone lower extremity DECT protocol with images of ankles and feet were included in the study. Then another database search of the period from January 2015 to December 2017 was performed to find a comparative group that underwent DECT gout protocol of ankles and feet region scanned at 80/140 kV. In order to more reliably observe the effects of the different dual energy voltage combination, 37 pairs of patients were matched for age, gender and serum uric acid level between the two groups for similar baseline characteristics. Patients with normal range of body mass index (18.50-24.99 kg/m^2) according to the World Health Organization/National Institutes of Health classification were only included since obesity could affect the radiation dose [21]. The diagnosis of gout was made by a physician who board certified in rheumatology with 18 years of experience. Patients with a total score of 8 or greater are classified as gout according to the ACR/EULAR 2015 classification criteria [14].

DECT acquisition technique

All CT examinations were performed with dual-source CT scanner in dual energy (DE) mode. The 80/150 Sn kV DECT examinations were obtained with a Somatom Force unit (Siemens Healthineers). Examination parameters used with the Force unit were as follows (Table 1): tube A: tube voltage of 80 kV and reference current-time product of 120 mAs; tube B: tube voltage of 150 Sn kV, where Sn indicates the use of a tin filter, reference current-time product of 80 mAs, rotation time of 0.5 s, pitch of 0.7 and collimation of 0.6 mm. The 80/140 kV DECT examinations were performed with a Somatom Definition unit (Siemens Healthineers). Examination parameters used with the Definition unit were as follows (Table 1): tube A: tube voltage of 80 kV, reference current-time product of 425 mAs; tube B: 140 kV, reference current-time product of 100 mAs, rotation time of 1.0 s, pitch of 0.7 and collimation of 0.6 mm. A real-time automatic tube current modulation software (CAREDose 4D; Siemens Healthineers) was used in both the protocols. Conventional linearly blended, virtual 120-kV axial, coronal, and sagittal CT reconstructions (thickness, 2 mm; increment, 2 mm; I70h kernel for the Definition data, Br69 kernel for the Force data) were obtained by using iterative reconstruction [SAFIRE (sinogram affirmed iterative reconstruction) for the Definition data, ADMIRE (adaptive model-based iterative reconstruction) for the Force data] for clinical reading.

Table 1 Settings for dual-energy computed tomography (DECT) gout protocol

	80/140 kV acquisition		80/150 Sn kV acquisition	
Scan parameters	Tube A	Tube B	Tube A	Tube B
Tube voltage (kV)	80	140	80	150 Sn
Pitch factor	0.7	0.7	0.7	0.7
Tube current–time product (mAs)	425	100	120	80
Rotation time (s)	1.0	1.0	0.5	0.5
Slice width (mm)	0.6	0.6	0.6	0.6
Reconstruction increment (mm)	2	2	2	2
DECT workstation settings				
Soft tissue (HU)	50		50	
Ratio	1.25		1.40	
Range	5		5	
Minimum/maximum (HU)	150/500		150/500	
Air distance/bone distance	5/10		5/10	

CTDIvol volume CT dose index, *150 Sn kV* 150 kV with additional tin filter (Sn)

For DE-specific analysis of gout, data were processed on a multimodality workstation with dedicated software (SyngoVia VB 10B; Siemens Healthineers) using a two-material decomposition algorithm. On this software, green pixels represent monosodium urate, blue outlines cortical bone and pink depicts trabecular or cancellous bone and these colour codes findings were fused onto the standard grey-scale CT images. Images are displayed in axial, coronal, and sagittal CT reconstructions (thickness, 2 mm; increment, 2 mm) and volume rendering 3D reconstructions. The workstation parameters of gout application were identical between the two CT systems, except for ratio setting since the ratio value changes according to the tube voltage combination. The detailed settings of the DECT workstation are listed in Table 1.

Evaluation of DECT artefacts

To identify and characterise artefacts, all DECT images were independently reviewed by two musculoskeletal radiologists with 6 and 10 years' experience on DECT of patients with suspected gout. Images were displayed digitally on monitors with a picture archiving and communication system (PACS) software (INFINITT Healthcare, Seoul, Korea). All personal and technical data has been removed from the images of both protocols. A total of 74 cases were displayed on the liquid-crystal display (LCD) in random order, regardless of the type of image protocol. In accordance with our clinical routine, reviewers were free to choose the appropriate planes—axial, sagittal or coronal—of colour-coded images. The types and number of artefacts observed were assessed by the two readers. In cases where there was disagreement between the readers, further discussion had been made to achieve consensus, considering medical records and results of ultrasonography if existed. Artefacts were defined by the criteria listed in Table 2, Figs. 1, 2, 3 and 4; these criteria are based on the observations of this study and others [5, 15, 17–19].

Evaluation of radiation dose

Radiation exposure was estimated by using the volume CT dose index (CTDIvol) and dose-length-product (DLP) for each patient. The DLP was provided automatically by the scanner system and is the product of the CTDIvol and the scan range (cm) for the complete length of the exposed volume. The effective dose was calculated for each scan by multiplying the DLP with the International Commission on Radiological Protection (ICRP) tissue weighting factor of 0.01 [mSv/(mGy·cm)] for bone surface [22].

Statistical analysis

The Shapiro-Wilk test was used for the normality test (p value greater than 0.05 indicated normal distribution of data) and Q-Q plot used as a backup. For quantitative data, comparison between the two matched groups was done using the paired t-test (if data were normally distributed) or the Wilcoxon signed-ranks test (if non-normally distributed parameters). For qualitative data, the McNemar's test was performed. Continuous variables are presented by either mean and standard deviation (for normal distribution) or median and interquartile interval (for non-normal distribution). Categorical variables were expressed as frequency (percentages). The significance level for all statistical tests was set at 5% and all tests were two-tailed. The κ statistic was used to assess inter-rater reliability between the two readers in the evaluation of artefact on DECT images. A κ value of 0.00–0.20, 0.21–0.40, 0.41–0.60, 0.61–0.80, or 0.81–1.00, indicated slight, fair, moderate, substantial or almost perfect, respectively [23]. Inter-rater agreement was measured by means of the overall proportion

Table 2 Artefacts in dual-energy computed tomography (DECT) gout protocol based on observations from this study and others

Type of artefact	Findings
Skin	Green colouring of the skin that is confined to the skin (Fig. 1a)
Nail bed	Green colouring of nails or nail beds that is confined to the nails or nail beds (Fig. 1b)
Submillimetre	Colouring of single pixels or areas smaller than 1 mm (Fig. 1c)
Beam hardening	Green colouring associated with metal objects or dense cortical bone (Fig. 1d)
Motion	Green colouring associated with patient's motion (Fig. 2)
Vascular	Green colouring associated with calcified vessels (Fig. 3)
Clumpy artefact along tendon	Diffuse pattern of green colouring along the tendon without symptom, and not identified abnormal echogenicity on ultrasonography (Fig. 4)

of agreement [24, 25]. Analyses were performed by using statistical software (SPSS Statistics for Windows version 21; IBM, Armonk, New York, USA)

Results

Patient characteristics for the two study groups are shown in Table 3. The groups were well-matched in terms of age, gender, laterality, serum uric acid, and the proportion of the gout patient.

When it comes to DECT artefacts, 80/150 Sn kV images had significantly fewer patients with artefacts, compared to 80/140 kV images. Eleven (30%) of 37 cases showed some form of artefact in the 80/150 Sn kV group, whereas 35 (94.6%) of 37 cases in the 80/140 kV group ($p < 0.001$). The types and incidences of each artefact in both groups are summarised in Table 4. Except for the motion artefact, the rest of the artefacts—skin, nail bed, submillimetre, motion, vascular, beam-hardening, clumpy artefact along tendon—were significantly less observed in the 80/150 Sn kV acquisitions. In particular, vascular artefact, beam-hardening artefact and clumpy artefact along tendon were not visible at all on the

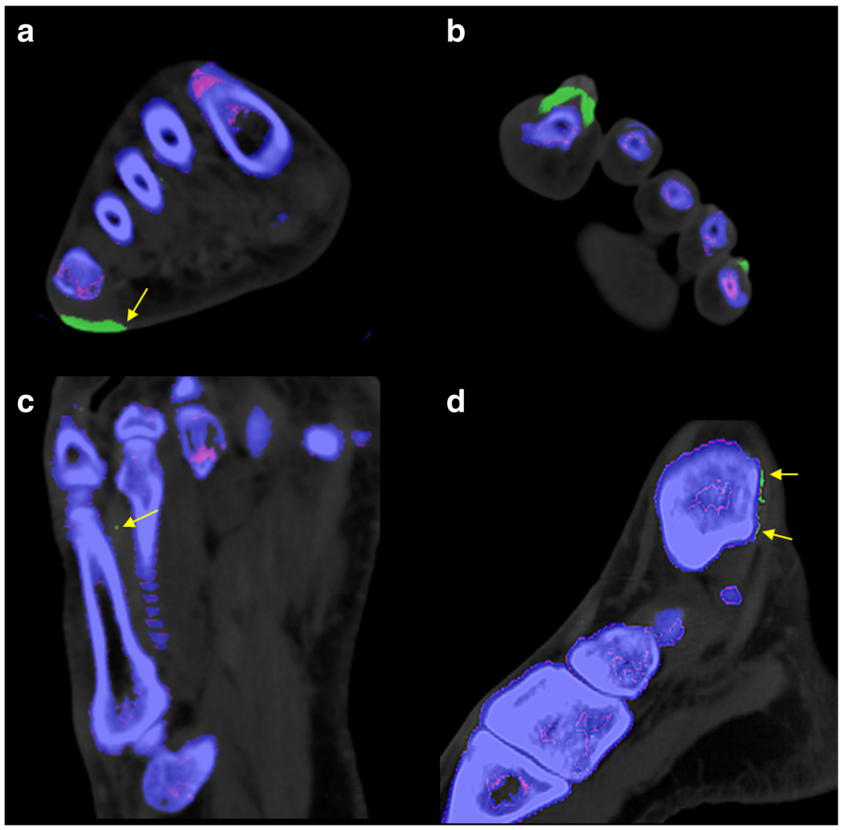

Fig. 1 Artefacts in dual-energy CT (DECT) gout protocol. **a** Skin artefact (*arrow*) is seen on coronal DECT image of 58-year-old man. **b** Nail bed artefacts (*arrows*) are visible in the first and fifth toes on coronal DECT image of 43-year-old man. **c** Submillimetre artefact (*arrow*) is seen on axial DECT image of 37-year-old man. **d** Beam-hardening artefact (*arrows*) from dense cortical bone is seen on sagittal DECT image along the posterior cortex of the distal fibula of 48-year-old man

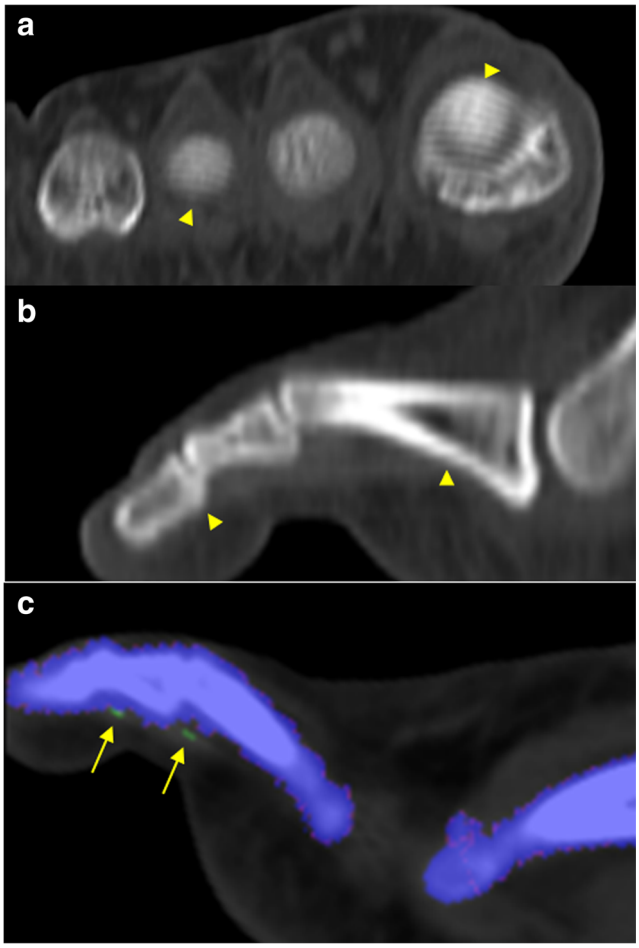

Fig. 2 Motion artefact (*arrowheads*) is seen on coronal (**a**) and sagittal (**b**) standard grey-scale CT images of 48-year-old man. Associated green colouring artefact (*arrows* in **c**) is visible on sagittal DECT image of the third toe

80/150 Sn kV DECT images (Table 4) (Fig. 5). The κ values showed substantial to almost perfect reliability (range, 0.71–1.0) for all types of DECT artefacts (Table 4). The inter-rater agreement exceeded 0.8 for all the artefacts (0.95 for skin; 0.96 for nail bed; 0.88 for submillimetre; 0.92 for motion; 1 for vascular; 0.92 for beam hardening; 0.93 for clumpy artefact along tendon).

Radiation dose was significantly reduced for the 80/150 Sn kV acquisitions in comparison to the 80/140 kV acquisitions (Table 5). On average, CTDIvol was 2.8 times higher for the 80/140 kV protocol (15.26 ± 2.84 mGy) when compared with the 80/150 Sn kV protocol (5.50 ± 0.99 mGy; $p < 0.001$). On average, DLP and effective dose were also reduced by a factor of 3.3 using the 80/150 Sn kV protocol in comparison to the 80/140 kV acquisitions (DLP: 104.46 ± 10.66 mGy·cm vs 344.70 ± 56.39 mGy·cm, $p < 0.001$; effective dose: 1.04 ± 0.11 mSv vs 3.45 ± 0.56 mSv, $p < 0.001$).

Discussion

The results of our study show that the 80/150 Sn kV voltage combination could be suggested as one of the artefact reduction methods of the DECT gout protocol when compared to the conventional 80/140 kV. In addition, applying 80/150 Sn kV voltage combination could lower radiation dose in gout protocol.

DECT has emerged as a non-invasive, accurate and reproducible method for detecting monosodium urate deposits in patients with suspected gout [6, 13, 15, 26–28]. Furthermore, Choi et al [27] reported that DECT was four times more

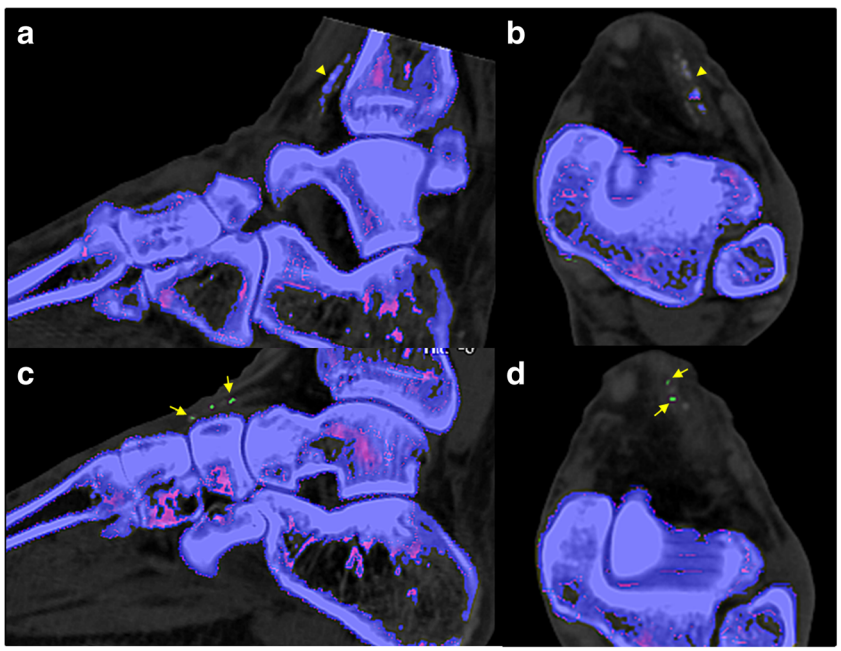

Fig. 3 Vascular artefact associated with calcified vessel on dual-energy CT (DECT) images of 76-year-old man. Calcified anterior tibial artery depicted with blue pixels (*arrowheads*) is seen on sagittal (**a**) and axial (**b**) DECT images. Associated green artefact (*arrows*) is visible on sagittal (**c**) and axial (**d**) DECT images

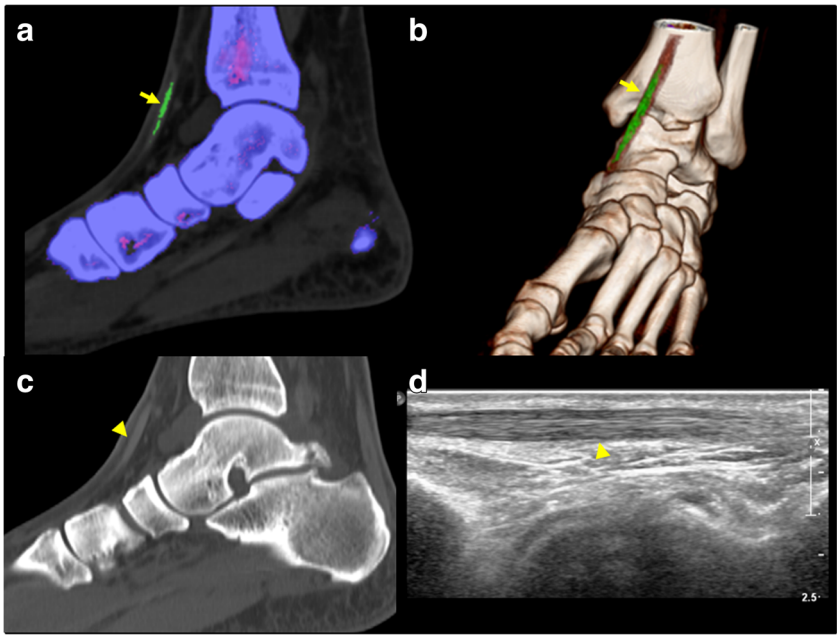

Fig. 4 Clumpy artefact along tendon on dual-energy CT (DECT) images of 31-year-old man. Diffuse pattern of green colouring along the tibialis anterior tendon (*arrows*) is visible on sagittal DECT (**a**) and 3D DECT reconstruction (**b**) images. Synovial fluid aspirate from the tibialis anterior tendon sheath was performed, but no urate crystal was identified under polarised microscopy. There was no evidence of crystal deposition within the tibialis anterior tendon (*arrowheads*) on sagittal standard grey-scale CT image (**c**) and ultrasound exam (**d**)

efficacious in identifying urate deposits than the clinical examination. Based on the high diagnostic performance proven with sufficient published data, DECT has been included in the 2015 gout classification criteria of the ACR/EULAR for the first time. The 2015 gout classification is organised into a total of eight domains—four clinical criteria, two laboratory criteria and two imaging criteria—that contribute weighted scores. The imaging criteria include evidence of urate deposition in a symptomatic joint and bursa on monosodium urate demonstration on DECT (0 or +4) or ultrasound images (double-contour sign on articular cartilage). The second imaging criterion is the presence of at least one gout-related erosion of the feet or hands on radiography characterised by cortical erosions with sclerotic margin and overhanging edge (0 or +4) [14]. Although DECT and ultrasound are both included for imaging evidence of urate deposition, ultrasound is operator-dependent and has lower detection rate if the urate is deep seated or the patient is obese. Therefore, the usefulness of DECT may be greater than ultrasound in terms of diagnostic performance.

However, DECT scanning and post-processing do produce artefacts which may result in false-positive findings in patients with suspected gout, if not recognised properly. The reported artefacts by far are nail bed, skin, submillimetre, beam hardening, vascular calcification, and tissues around arthroplasties such as osteoarthritis [1–3, 17–19]. Nail bed and skin artefacts may be due to the overlap of DECT values of MSU and the

Table 3 Clinical characteristics of both the 80/150 Sn kV and 80/140 kV groups

	Group		*p* value
	80/150 Sn kV (*n* = 37)	80/140 kV (*n* = 37)	
Sex			1
male	37	37	
Laterality			1
right	17	17	
left	20	20	
Age (years) [a]	48.97 ± 14.57	49.46 ± 14.69	0.53
BMI (kg/m^2)	22.33 ± 0.92	21.46 ± 1.01	0.47
Uric acid (mg/dl)	7.21 ± 1.78	7.55 ± 1.91	0.06
Diagnosis of gout [b]			0.34
yes	25	21	
no	12	16	

BMI body mass index

[a] Data are the mean ± standard deviation

[b] If the total score was ≥8, classified as gout according to the ACR / EULAR 2015 classification criteria

Table 4 The types and incidences of each artefact in both the 80/150 Sn kV and 80/140 kV groups

Type of Artefact	Group		*p* value	κ
	80/150 Sn kV (*n* = 37)	80/140 kV (*n* = 37)		
Skin			<0.001	0.93
Absence	36	20		
Presence	1	17		
Total no. of artefacts	1	45		
Nail bed			<0.001	0.92
Absence	31	5		
Presence	6	32		
Total no. of artefacts	6	79		
Submillimetre			<0.001	0.71
Absence	33	16		
Presence	4	21		
Total no. of artefacts	6	52		
Motion			0.304	0.84
Absence	36	34		
Presence	1	3		
Total no. of artefacts	1	5		
Vascular			0.314	1.0
Absence	37	36		
Presence	0	1		
Total no. of artefacts	0	1		
Beam hardening from dense cortical bone			0.011	0.72
Absence	37	31		
Presence	0	6		
Total no. of artefacts	0	6		
Clumpy artefact along tendon			<0.001	0.81
Absence	37	21		
Presence	0	16		
Total no. of artefacts	0	29		

keratin. Scattered foci of submillimetre urate-like pixels in a non-anatomic distribution are typically regarded as image noise. Beam-hardening from metal objects or dense cortical bone can cause spurious pixel mimicking urate deposits. Patient motion during the scan can also result in image distortion and artefacts. Urate-like pixels in calcified vessels has been described in some reports and it is thought that noise within small structures may contribute to vascular artefact [17–19]. Like the previous reports, the most commonly encountered artefact was in the nail beds which can be seen in 51.35% (38/74) of patients in our study. Other types of artefact including skin, submillimetre specks, beam hardening, vascular and motion were also observed as reported in previous studies.

The clumpy artefact along tendon observed in the present study is a type of DECT artefact which has not yet been reported (Fig. 4). A total of 29 clumpy artefacts were found within the tendons—tibialis anterior (*n* = 9), Achilles (*n* = 9), tibialis posterior (*n* = 5), peroneal (*n* = 3), extensor hallucis longus (*n* = 2), flexor digitorum longus (*n* = 2) and extensor digitorum longus (*n* = 1)—in the 16 patients of the 140/80 kV group. These "green-colouring" tendons showed normal echogenicity on the additional ultrasound exam. Among three of them (two in tibialis anterior tendons, one in Achilles tendon), synovial fluid aspirate from the tendon sheath was performed, but no MSU crystal was identified under polarised microscopy. In 2011, Glazebrook et al [15] have explained that even though tiny scattered green pixelation within tendons are artefact caused by image noise, more clumped areas of green pixelation within tendons may be the result of subclinical deposition of uric acid. However, the fact that ultrasonographic changes such as inhomogeneous tendons and intratendinous hyperechoic bands suggesting tendon involvement in clinically asymptomatic gout patients [29] were not observed in additional ultrasonography and that this phenomenon was found only at 140/80 kV DECT scan indicate that

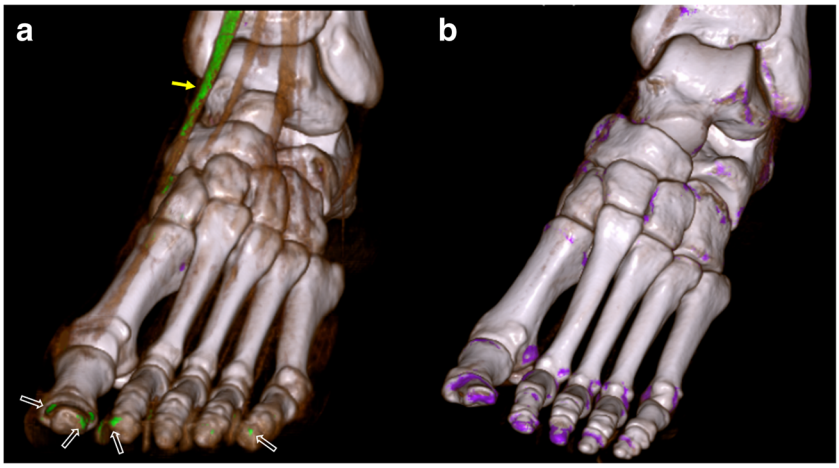

Fig. 5 Three-dimensional reformatted dual-energy CT (DECT) images of two patients with suspected gout. (Serum uric acid was 7.8 mg/dl and 7.6 mg/dl, respectively.) Neither patient was classified as gout according to the ACR / EULAR 2015 classification criteria. **a** DECT acquisition using voltage combination 80kV and 140 kV in a 32-year-old man (CTDIvol = 16.94 mGy; DLP = 346 mGy·cm). **b** DECT acquisition using 80kV and 150 kV with additional tin filter (Sn) in a 33-year-old man (CTDIvol = 4.87 mGy; DLP = 95.6 mGy·cm). Nail bed artefacts (*open arrows*) and clumpy artefact along tendon (*solid arrow*) were observed in the 80/140 kV scan (**a**), whereas no artefact was shown in the 80/150 Sn kV scan (**b**). Furthermore, a more than three-fold dose reduction was achieved with the 80/150 Sn kV acquisition

the clumped pattern of green pixilation within tendon we defined is an artefact.

There have been various technical efforts to reduce artefact in DECT. Physical patient adjustments, such as taping a patient's limb to decrease movement, or increasing gantry speeds can be used to decrease motion artefacts. Use of manufacturer's recommended specialised kernel or reconstruction algorithm can be used to improve image quality, decrease noise and artefacts. Adjustment of parameter settings of the DECT workstation, such as dual-energy ranges, air and bone distance, can help provide optimal image quality [2, 3, 16–19]. In addition to these tactics, application of 80/150 Sn kV voltage combination in dual-source DECT system could also be used to optimise image quality, decrease artefacts, and more accurately identify the presence of urate deposits for DECT gout protocol.

In dual-source CT systems, applying additional tin filter to the high-kV beam can improve dual-energy spectral separation. Several studies have demonstrated that dual-energy material discrimination can be improved by means of tin filter in DSCT [20, 30–32]. Krauss et al [20] found that the performance of DECT was best for 80/150 Sn kV and worst for 80/140 kV among the various tube voltage combinations—80/140 kV, 80/140 Sn kV, 100/140 Sn kV, 80/150 Sn kV, 90/150 Sn kV, 100/150 Sn kV. This was closely related to the fact that image noise was highest for the voltage combination 80/140 kV and lowest for 80/150 Sn kV. Since the large number of artefacts in DECT gout protocol are caused by image noise, the significant artefact reduction observed at 80/150 Sn kV group in this study would be affected by superior dual-energy performance of the 80/150 Sn kV voltage combination.

In this study, we demonstrated that 150 kV with tin filtration reduced radiation dose by a factor of 2.8 (for CTDIvol) and 3.3 (for DLP and effective dose), compared to 140kV without tin filtration at the same low-voltage beam of 80 kV. This finding is in concordance with the recent clinical studies revealing that unenhanced CT performed at 150 kV with spectral shaping by a tin filter substantially lowers patient exposure than using lower kV settings (100-140 kV) without additional spectral shaping of the X-ray beam [33, 34]. Furthermore, some studies suggested that the use of tin filter in DECT has reduced radiation dose to the level similar to single-energy CT [32, 35]. An additional tin filter allows for spectral shaping by removing the bulk of the lower energy photons that does not exit the patient and raising the mean photon energy of the applied radiation, thus increasing a rate of dose-efficient photons from the spectrum [36]. In this study, there was quite a

Table 5 Radiation exposure parameters

	80/150 Sn kV	80/140 kV	*p* value
CTDIvol (mGy) [a]	5.27 (4.94, 5.60) (min, 4.61; max, 8.90)	16.50 (15.24, 17.76) (min, 7.20; max, 17.07)	<0.001
DLP (mGy·cm) [b]	104.46 ± 10.66 (min, 83.; max, 125.30)	344.70 ± 56.39 (min, 257; max, 466)	<0.001
Effective dose (mSv)[b]	1.04 ± 0.11 (min, 0.84; max, 1.25)	3.45 ± 0.56 (min, 2.57; max, 4.66)	<0.001

[a] Data are medians; *numbers in parentheses* are interquartiles

[b] Data are the mean ± standard deviation

difference between the reference tube current–time product for high-kV beam (425 mAs for 140 kV, 120 mAs for 150 Sn kV). Using tin-filtered 150 kV, it was possible to get adequate image quality even at the low reference mAs (due to spectral shaping of the X-ray beam), so the lower reference mAs was set for the Force machine. Therefore, the lower reference mAs may have the additional effect on dose reduction, but that extra effect could also be part of what we can get with tin filter.

Giving increasing prevalence of the gout and the fact that patients often suffer from recurrent gout attacks [37] makes the "ALARA" (as low as reasonably achievable) principle particularly important. In this context, taking advantage of 80/150 Sn kV voltage combination would facilitate low-dose technique for DECT imaging to reduce cumulative radiation dose. Hence, the protocol is especially suitable for patients with chronic course of gout who requiring follow-up examinations for monitoring the effect of urate-lowering therapy.

Our study has some limitations. First, as the scans were performed on two different CT systems, it may not allow for an exact comparison due to differences in the data measurement systems such as versions of reconstruction kernel and iterative reconstruction (IR) of both CT scanners. For example, the Model Based Iterative Reconstruction algorithm, called ADMIRE, was developed as a more advanced noise reduction method than traditional IR algorithm, which may have contributed to the superior artefact reduction of the Force unit [38, 39]. However, given the results of previous phantom study, it is clear that the noise level depends on the selected DE voltage combination and tin filtration in DSCT [20]. Therefore, the lowest image noise observed at 80/150 Sn kV can be assumed to be related to artefact elimination (either alone or with other factors). Nevertheless, we acknowledge that different scanner settings might be act as a confounder of image quality. Further prospective studies performed using one dual-source CT system (Somatom Force) would be warranted to consolidate our findings. Second, although all image information was completely removed from all images and the analysis of the two protocols was performed in a random order, we acknowledge that the readers might have recognised the different protocols due to their slightly different image appearance. Thus, our results regarding artefact evaluation might be influenced by a cognitive recognition bias. By applying strict and consistent analysis criteria to all DECT images, the readers tried to minimise this bias. Third, not all clumpy artefacts of tendon were confirmed by fluid aspirate and polarised light microscopy, because there were not sufficient clinical signs—such as swelling, pain or tenderness around the tendon—that could justify the risk of invasive testing. However, as mentioned earlier, the facts that despite of clinical similarity between the two groups of patients this phenomenon was observed only at 80/140kV protocol and that the additional ultrasound did not reveal any ultrasonographic changes suggestive of gouty arthritis in tendon would indicate that this clumpy colour-coded pattern of tendon could be regarded as an artefact. Fourth, to maintain consistency of the assessment of DECT images, only foot and ankle areas were evaluated in patients with suspected gout. Thus, there is a possibility that the detailed results might be different, if the assessment were extended to the other extremities such as hand and wrist. However, the mainstream results of this study would not be impaired. Fifth, there was difference in the tube current condition between the 80/140kV and 80/150 Sn kV groups, as a lower reference tube current-time product (mAs) was set for the 150 Sn kV. Even if the lower reference mAs could be part of the effect we can get with tin filter, this might have a confounding effect on dose reduction.

In conclusion, the 80/150 Sn kV voltage combination in dual-source DECT system could be used as one of the artefact reduction methods while reducing radiation dose for gout protocol when compared to the conventional 80/140 kV. Therefore, DE acquisition using 80/150 Sn kV could facilitate its diagnostic performance in the patients with suspected gout and improve the utility of DECT for monitoring the effect of urate-lowering therapy in patients with recurrent gout.

Acknowledgements This work was supported by the Gachon University research fund of 2017 (GCU-2017-5259).

Funding This study has received funding by the Gachon University Research Center, Incheon, South Korea (GCU-2017-5259).

Compliance with ethical standards

Guarantor The scientific guarantor of this publication is Ji Young Jeon, M.D.

Conflict of interest The authors of this manuscript declare no relationships with any companies, whose products or services may be related to the subject matter of the article.

Statistics and biometry No complex statistical methods were necessary for this paper.

Informed consent Written informed consent was waived by the Institutional Review Board.

Ethical approval Institutional Review Board approval was obtained.

Methodology
- retrospective
- case-control study/observational
- performed at one institution

References

1. Fritz J, Henes JC, Fuld MK, Fishman EK, Horger MS (2016) Dual-energy computed tomography of the knee, ankle, and foot:

noninvasive diagnosis of gout and quantification of monosodium urate in tendons and ligaments. Semin Musculoskelet Radiol 20: 130–135
2. Omoumi P, Verdun FR, Guggenberger R, Andreisek G, Becce F (2015) Dual-energy CT: basic principles, technical approaches, and applications in musculoskeletal imaging (Part 2). Semin Musculoskelet Radiol 19:438–445
3. Nicolaou S, Liang T, Murphy DT, Korzan JR, Ouellette H, Munk P (2012) Dual-energy CT: a promising new technique for assessment of the musculoskeletal system. AJR Am J Roentgenol 199:S78–S86
4. Johnson TRC (2012) Dual-energy CT: general principles. AJR Am J Roentgenol 199:S3–S8
5. Johnson T, Fink C, Schönberg SO, Reiser MF (2011) Dual energy CT in clinical practice, 1st edn. Springer, Berlin Heidelberg
6. Nicolaou S, Yong-Hing CJ, Galea-Soler S, Hou DJ, Louis L, Munk P (2010) Dual-energy CT as a potential new diagnostic tool in the management of gout in the acute setting. AJR Am J Roentgenol 194:1072–1078
7. van Elmpt W, Landry G, Das M, Verhaegen F (2016) Dual energy CT in radiotherapy: current applications and future outlook. Radiother Oncol 119:137–144
8. Coupal TM, Mallinson PI, Munk PL, McLaughlin P, Ouellette HA (2015) Latest advances in musculoskeletal dual energy computed tomography (DECT). Curr Radiol Rep 3:23
9. Khanduri S, Goyal A, Singh B et al (2017) The utility of dual energy computed tomography in musculoskeletal imaging. J Clin Imaging Sci 7:34
10. Flohr TG, McCollough CH, Bruder H et al (2006) First performance evaluation of a dual-source CT (DSCT) system. Eur Radiol 16:256–268
11. Ogdie A, Taylor WJ, Weatherall M et al (2014) Imaging modalities for the classification of gout: systematic literature review and meta-analysis. Ann Rheum Dis 74:1868–1874
12. Bongartz T, Glazebrook KN, Kavros SJ et al (2014) Dual-energy CT for the diagnosis of gout: an accuracy and diagnostic yield study. Ann Rheum Dis 74:1072–1077
13. Choi HK, Burns LC, Shojania K et al (2012) Dual energy CT in gout: a prospective validation study. Ann Rheum Dis 71:1466–1471
14. Neogi T, Jansen T, Dalbeth N et al (2015) 2015 Gout classification criteria: an American College of Rheumatology/European League Against Rheumatism collaborative initiative. Arthritis Rheumatol 67:2557–2568
15. Glazebrook KN, Guimaraes LS, Murthy NS et al (2011) identification of intraarticular and periarticular uric acid crystals with dual-energy CT: initial evaluation. Radiology 261:516–524
16. Tashakkor AY, Wang JT, Tso D, Choi HK, Nicolaou S (2012) Dual-energy computed tomography: a valid tool in the assessment of gout? Int J Clin Rheumtol 7:73
17. Mallinson PI, Coupal T, Reisinger C et al (2014) Artifacts in dual-energy CT gout protocol: a review of 50 suspected cases with an artifact identification guide. AJR Am J Roentgenol 203:W103–W109
18. Chou H, Chin TY, Peh WCG (2017) Dual-energy CT in gout—a review of current concepts and applications. J Med Radiat Sci 64: 41–51
19. Coupal TM, Mallinson PI, Gershony SL et al (2016) Getting the most from your dual-energy scanner: recognizing, reducing, and eliminating artifacts. AJR Am J Roentgenol 206:119–128
20. Krauss B, Grant KL, Schmidt BT, Flohr TG (2015) The importance of spectral separation: an assessment of dual-energy spectral separation for quantitative ability and dose efficiency. Invest Radiol 50: 114–118
21. Boos J, Lanzman RS, Heusch P et al (2016) Does body mass index outperform body weight as a surrogate parameter in the calculation of size-specific dose estimates in adult body CT? Br J Radiol 89: 20150734
22. Wrixon AD (2008) New ICRP recommendations. J Radiol Prot 28: 161–168
23. Landis JR, Koch GG (1977) An application of hierarchical kappa-type statistics in the assessment of majority agreement among multiple observers. Biometrics:363–374
24. Kim H-Y (2013) Statistical notes for clinical researchers: evaluation of measurement error 2: Dahlberg's error, Bland-Altman method, and Kappa coefficient. Restor Dent Endod 38:182–185
25. Kottner J, Audige L, Brorson S et al (2011) Guidelines for Reporting Reliability and Agreement Studies (GRRAS) were proposed. J Clin Epidemiol 64:96–106
26. Desai MA, Peterson JJ, Garner HW, Kransdorf MJ (2011) Clinical utility of dual-energy CT for evaluation of tophaceous gout. Radiographics 31:1365–1375
27. Choi HK, Al-Arfaj AM, Eftekhari A et al (2009) Dual energy computed tomography in tophaceous gout. Ann Rheum Dis 68:1609–1612
28. Dalbeth N, Aati O, Gao A et al (2012) assessment of tophus size a comparison between physical measurement methods and dual-energy computed tomography scanning. J Clin Rheumatol 18:23–27
29. Pineda C, Amezcua-Guerra LM, Solano C et al (2011) Joint and tendon subclinical involvement suggestive of gouty arthritis in asymptomatic hyperuricemia: an ultrasound controlled study. Arthritis Res Ther 13:R4
30. Primak A, Ramirez Giraldo J, Liu X, Yu L, McCollough CH (2009) Improved dual-energy material discrimination for dual-source CT by means of additional spectral filtration. Med Phys 36:1359–1369
31. Stolzmann P, Leschka S, Scheffel H et al (2010) Characterization of urinary stones with dual-energy CT: improved differentiation using a tin filter. Invest Radiol 45:1–6
32. Primak AN, Giraldo JCR, Eusemann CD et al (2010) Dual-source dual-energy CT with additional tin filtration: dose and image quality evaluation in phantoms and in vivo. AJR Am J Roentgenol 195: 1164–1174
33. Kim CR, Jeon JY (2018) Radiation dose and image conspicuity comparison between conventional 120 kVp and 150 kVp with spectral beam shaping for temporal bone CT. Eur J Radiol 102: 68–73
34. Dewes P, Frellesen C, Scholtz J-E et al (2016) Low-dose abdominal computed tomography for detection of urinary stone disease− Impact of additional spectral shaping of the X-ray beam on image quality and dose parameters. Eur J Radiol 85:1058–1062
35. Henzler T, Fink C, Schoenberg SO, Schoepf UJ (2012) Dual-energy CT: radiation dose aspects. AJR Am J Roentgenol 199: S16–S25
36. Haubenreisser H, Meyer M, Sudarski S, Allmendinger T, Schoenberg SO, Henzler T (2015) Unenhanced third-generation dual-source chest CT using a tin filter for spectral shaping at 100kVp. Eur J Radiol 84:1608–1613
37. Monu JU, Pope TL Jr (2004) Gout: a clinical and radiologic review. Radiol Clin North Am 42:169–184
38. Kuya K, Shinohara Y, Kato A, Sakamoto M, Kurosaki M, Ogawa T (2017) Reduction of metal artifacts due to dental hardware in computed tomography angiography: assessment of the utility of model-based iterative reconstruction. Neuroradiology 59:231–235
39. Boudabbous S, Arditi D, Paulin E, Syrogiannopoulou A, Becker C, Montet X (2015) Model-based iterative reconstruction (MBIR) for the reduction of metal artifacts on CT. AJR Am J Roentgenol 205: 380–385